

## Shape evolution in the transitional gadolinium, dysprosium, erbium, and ytterbium nuclei

J. Dudek

*Centre de Recherches Nucléaires, F-67037 Strasbourg Cedex, France*

W. Nazarewicz\*

*Department of Mathematical Physics, Lund Institute of Technology,*

*S-22007 Lund, Sweden*

(Received 25 June 1984)

Shape evolution in the  $I \geq 30\hbar$  high-spin states of  $^{144-150}\text{Gd}$ ,  $^{150-156}\text{Dy}$ ,  $^{152-158}\text{Er}$ , and  $^{154-160}\text{Yb}$  is predicted theoretically within the cranking approximation using the generalized Strutinsky method. A comparison with available experimental data is provided.

The high-spin behavior of atomic nuclei is in general very strongly influenced by the alignment of individual nucleonic angular momenta along the axis of rotation. The shape polarization of the nucleonic orbitals is ultimately related to this effect and provides a straightforward link between the individual alignments and the shape changes in the whole nucleus. In the *quantitative* description of the shape evolution, a carefully tested single-particle spectrum thus plays a very important role.

In order to study the shape properties at high spin we applied the Strutinsky-cranking method<sup>1-6</sup> together with the important extensions<sup>7-9</sup> which allow us to keep track of separate rotational bands characterized by parity  $\pi$  and signature  $r$ . Thus, the total energies are calculated as functions of deformations  $\beta_2$  and  $\gamma$  at each spin value  $I$  for the lowest-lying  $(\pi, r)$  configurations. In this respect we differ from earlier calculations<sup>3-6</sup> where the total energy surfaces correspond generally to the mixture of bands having different parities and signatures. Details about the method are to be found in Ref. 10; parameters of the Woods-Saxon potential are from Ref. 11.

In the present work we aim at a quantitative or at least a semiquantitative description. For this purpose it is important to test the single-particle potential on the high-spin data available from experimental discrete spectroscopy. In order not to test the quality of the single-particle spectra *simultaneously* with the adequacy of the cranking model approach we selected a few noncollectively rotating nuclei for a preliminary check. In those nuclei the total angular momenta are nearly parallel to the nuclear symmetry axis and the generalized Strutinsky approach reduces there to particle-hole analysis. Consequently, the (multi) particle-hole structure of the excitation probes primarily the single-particle spectrum generated by the deformed potential. Those results describe well the known experimental data and are the subject of a separate article.

In the following we present detailed theoretical predictions on the shape coexistence and shape evolution at high spins. The pairing effect is ignored since, for  $I > 30\hbar$ , it should play only a minor role. We should like to emphasize that (a) the results do not depend on any free parameter adjusted to any data on the discussed  $^{144-150}\text{Gd}$ ,  $^{150-156}\text{Dy}$ ,  $^{152-158}\text{Er}$ , and  $^{154-160}\text{Yb}$  nuclei, and (b) the reliability of the results depends on the correct theoretical description of the single-particle orbitals since the alignment process depends

sensitively on details of the single particle spectra.

*The  $^{144-150}\text{Gd}$  nuclei.* The results for  $^{144-150}\text{Gd}$  (Fig. 1) are characteristic for their extremely low appearance of superdeformed bands similarly as in modified oscillator calculations of Ref. 6. On a microscopic level this results from the well-pronounced proton gap  $Z = 64$  at *very large deformation*<sup>12,13</sup> (not to be confused with the experimentally observed  $Z = 64$  opening of  $\Delta E \sim 2.4$  MeV at spherical shape) which persists up to very high rotational frequencies. The competition between irregular deexcitation pattern and triaxial collective bands deserves noting. To our knowledge no experimental data for these nuclei at spins high enough are available at present.

*The  $^{150-156}\text{Dy}$  nuclei.* The results for  $^{150-156}\text{Dy}$  nuclei in Fig. 2 can already be partially confirmed by existing experimental data from quasicontinuum spectroscopy. The calculated rigid-body values for the moments of inertia of the  $^{152}\text{Dy}$  superdeformed band,  $2J = 165\hbar^2 \text{ MeV}^{-1}$ , compares rather well with the results  $2J \approx 167\hbar^2 \text{ MeV}^{-1}$  of Ref. 14 and  $2J \approx (170 \pm 4)\hbar^2 \text{ MeV}^{-1}$  of Ref. 15.

A discrete spectroscopy measurement<sup>16</sup> for  $^{154}\text{Dy}$  indicates a collective rotation pattern at relatively low spins ( $I \leq 32\hbar$ ), in agreement with the calculation. A clear onset of structural changes in the spectrum takes place at  $I \sim (31-33)\hbar$ . This corresponds to the presence of the low-lying series of states with  $\gamma = 60^\circ$  configurations (cf. Fig. 2) very close ( $\sim 600$  keV) to the yrast line already at  $I \sim (34-36)\hbar$ . The latter result agrees better with the experimental data than the results of Ref. 9, in which the modified oscillator potential was employed. According to our calculations the first yrast oblate shape configuration has  $I^\pi = 41^-$ .

A characteristic feature of the results discussed until now is the decreasing importance of the  $\gamma = 60^\circ$  particle-hole configurations when the neutron number varies from 84 to 90 and the growing distance from the superdeformed band relative to yrast. This is related to the occurrence of the  $N = 86$  gap which corresponds to superdeformed shape at  $\beta_2 \sim 0.6$ ,  $\gamma \sim 0^\circ$  and strongly contributes to the lowering of the superdeformed bands in the  $N = 86$  and a few neighboring isotones (see also Ref. 12). Also characteristically, in the spin range  $I \sim (30-50)\hbar$  the properties of  $^{156}\text{Dy}$  are predicted to differ distinctly from those of  $^{152}\text{Dy}$  and  $^{154}\text{Dy}$ ; in  $^{156}\text{Dy}$  there are almost no  $\gamma = 60^\circ$  configuration states close to the yrast line (cf. also Ref. 17). In this respect,

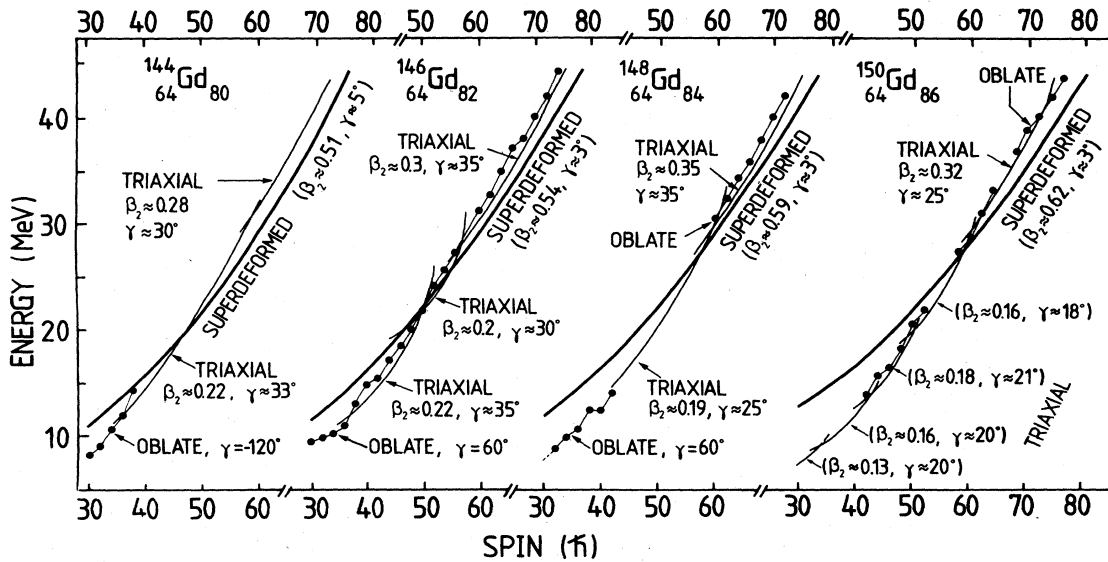


FIG. 1. Results of cranking model calculations on the high-spin behavior of  $^{144-150}\text{Gd}$ . The low-lying well-pronounced superdeformed band especially in  $^{144}\text{Gd}_{80}$  deserved noting. Pairing is ignored. Here, only the states with total parity  $\pi = \pi(\text{protons})\pi(\text{neutrons}) = +1$  and the total signature  $r = r(\text{protons})r(\text{neutrons}) = 1$  are displayed. It has been checked, however, that these results are representative for the shape evolution in most of the structures with the remaining parity-signature combinations, i.e.,  $r = \pm 1, \pi = \pm 1$ .

similarities are expected for  $^{152}\text{Dy}$  and  $^{154}\text{Dy}$ . Our calculations predict crossing between the two prolate bands in  $^{156}\text{Dy}$  at  $I \sim 38\hbar$  (Fig. 2), thus, explaining the irregularity observed<sup>17</sup> just above  $I^\pi = 38^+$  state. In  $^{150}\text{Dy}$  a triaxial band and a superdeformed band are very close together and appear at relatively higher spins. In calculations of Refs. 5 and 6 superdeformed bands in neutron deficient Dy nuclei become yrast at spins  $I \sim 45-55\hbar$  which is about  $10\hbar$  lower as compared to the results of the present study.

The  $^{152-158}\text{Er}$  nuclei. In the  $^{152-158}\text{Er}$  nuclei (Fig. 3) the su-

perdeformed bands begin at relatively higher spin values, as compared to the analogous isotones of Dy and, even more clearly, Gd. The two lighter Er isotopes are expected to remain oblate up to relatively high spins of  $I \sim 40\hbar$  and  $I \sim (44-46)\hbar$ , respectively (cf. Fig. 3). On the contrary,  $^{156}\text{Er}$  should clearly undergo a shape change from collective to oblate structures at the relatively low spin  $I \approx (30/32)\hbar$  (see also Refs. 5 and 6). Such a shape transition in  $^{156}\text{Er}$  has, in fact, been recently observed<sup>18</sup> at spins  $I > 32\hbar$  and confirmed<sup>19</sup> by the existence of the long feeding times in

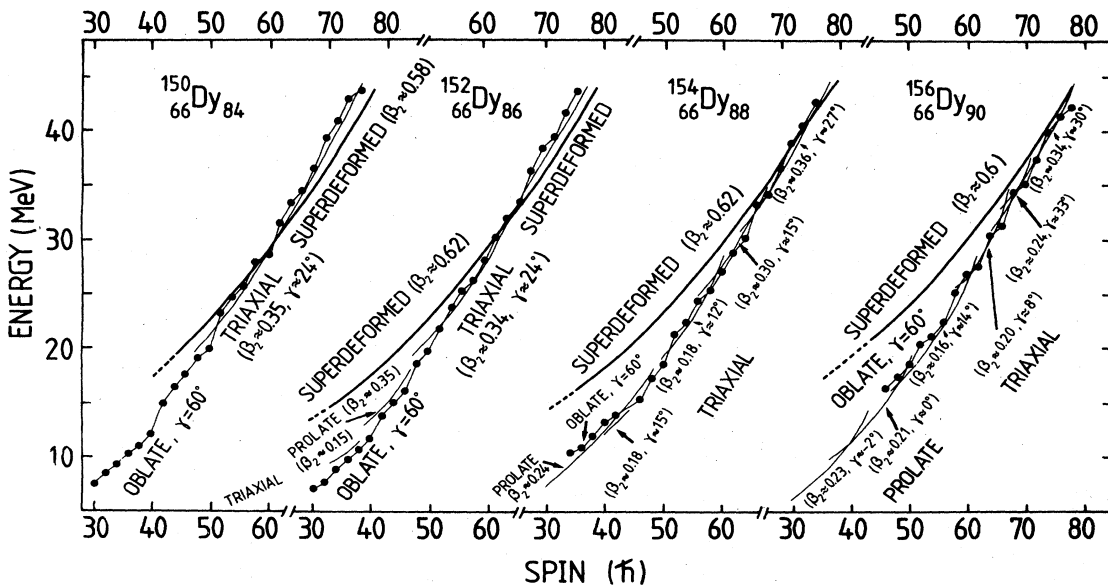


FIG. 2. Similar to that in Fig. 1 but for  $^{150-156}\text{Dy}$ . The predicted differences in the high-spin behavior between  $^{154}\text{Dy}$  and  $^{156}\text{Dy}$  are worth noting.

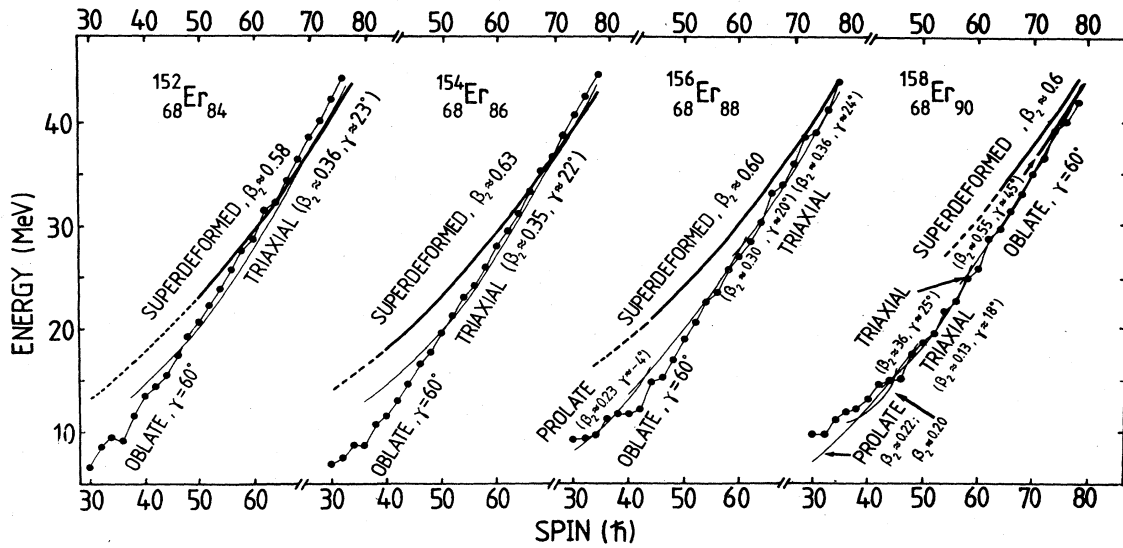


FIG. 3. Similar to that in Fig. 1 but for  $^{152-158}\text{Er}$ . Here, the behavior of  $^{152-154}\text{Er}$  is expected to be markedly different from that of  $^{156-158}\text{Er}$ , at least in the  $30\hbar \leq I \leq 45\hbar$  spin range.

the pre-yrast region of  $^{156}\text{Er}$  around spin  $30-50\hbar$ . The heaviest isotope  $^{158}\text{Er}$  is expected to undergo a transition from a collective to a  $\gamma = 60^\circ$  regime at  $I \geq 42\hbar$ . The calculated yrast line in  $^{158}\text{Er}$  has a rather complicated structure around  $I \sim 40\hbar$ . The crossing between the two prolate bands is expected between  $I = 38\hbar$  and  $I = 40\hbar$ . For  $I = 44\hbar$  the first noncollective state becomes yrast. Similarly as in Ref. 9, the  $I^\pi = 46^+$  state is very much favored in energy. These theoretical predictions seem to be in agreement with Simpson *et al.*,<sup>20</sup> who observed a characteristic change in the structure of the decay scheme for just  $I \geq 40\hbar$ .

*The  $^{154-160}\text{Yb}$  nuclei.* The onset of superdeformed configurations corresponds to  $I \sim (30-40)\hbar$  in  $^{156-158}\text{Yb}$ ; in  $^{154}\text{Yb}$  superdeformation exists at  $I \leq 46$  while in  $^{160}\text{Yb}$  at  $I \sim 70\hbar$  only. A very interesting feature of moderately high-spin configurations is a band-termination effect ( $^{158-160}\text{Yb}$ ) con-

sisting of a smooth shape evolution from a prolate collective to an oblate noncollective modes. Such an effect differs qualitatively from a band crossing effect; it has been discussed in Refs. 8, 9, and 21, while the results of Ref. 22 seem to provide an experimental evidence in  $^{158}\text{Yb}$  (details are to be found in Ref. 23).

In all the nuclei considered here there is a competition between the noncollective and triaxial bands at the high-spin region above  $I \geq 40\hbar$ . The deformation in the triaxial configurations increases gradually from ( $\beta_2 \approx 0.2, \gamma \approx 15^\circ$ ) to ( $\beta_2 \approx 0.4, \gamma \approx 25^\circ$ ) with increasing spin. This is related to the increasing effect of the characteristic high- $j$  low- $\Omega$  orbitals originating from the  $\pi i_{13/2}$  and  $\nu j_{15/2}$  shells. The energies of those orbitals quickly decrease with both the quadrupole deformation and rotational frequency, and the corresponding single-particle Routhians cross the Fermi levels

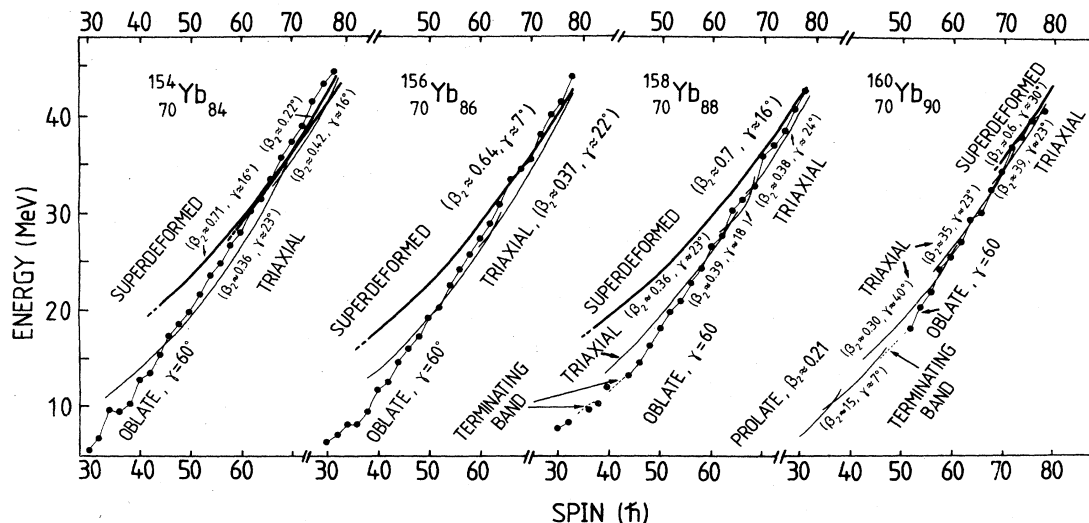


FIG. 4. Similar to that in Fig. 1 but for  $^{154-160}\text{Yb}$ ; the shape evolution leading to a band termination mechanism in  $^{158-160}\text{Yb}$  deserves noting.

above  $I \sim 50\hbar$ . The related local minima are rather well-defined and the corresponding motion differs characteristically from the band-termination picture.

Finally, we would like to point out that some of the lower spin ( $30\hbar \leq I \leq 40\hbar$ ) states represented in Figs. 1-4 are likely to lie even lower due to residual pairing correlations still present, especially in the proton systems.

In summary, with the carefully tested single-particle spectra of the deformed Woods-Saxon potential and using the cranking model, detailed predictions of the band crossings and deformation changes in 16 transitional rare earth nuclei have been made. Comparison with the experimental data

available at present on only a few nuclei shows good agreement with the theoretical calculations, and we hope that the presented predictions can be useful for the coming experimental studies.

We would like to thank T. Bengtsson and I. Ragnarsson for letting us use the configuration controlling routines of their modified oscillator code in our Woods-Saxon calculations. One of us (W.N.) acknowledges support from the Swedish Natural Science Research Council in the form of a postdoctoral fellowship in Lund.

\*On leave of absence from the Institute of Physics, Technical University, PL-00-662 Warsaw, Poland.

<sup>1</sup>R. Bengtsson *et al.*, Phys. Lett. **57B**, 301 (1975).

<sup>2</sup>K. Neergård *et al.*, Phys. Lett. **59B**, 218 (1975).

<sup>3</sup>G. Andersson *et al.*, Nucl. Phys. **A268**, 205 (1976).

<sup>4</sup>K. Neergård *et al.*, Nucl. Phys. **A262**, 61 (1976).

<sup>5</sup>C. G. Andersson *et al.*, Phys. Scr. **25**, 23 (1982).

<sup>6</sup>S. Åberg, Phys. Scr. **25**, 23 (1982).

<sup>7</sup>I. Ragnarsson *et al.*, Phys. Scr. **24** 215 (1981).

<sup>8</sup>T. Bengtsson and I. Ragnarsson, Phys. Lett. **115B**, 431 (1982); Nucl. Phys. A (to be published).

<sup>9</sup>T. Bengtsson and I. Ragnarsson, Phys. Scr. **T5**, 165 (1983).

<sup>10</sup>W. Nazarewicz *et al.*, Nucl. Phys. A (to be published).

<sup>11</sup>J. Dudek *et al.*, Phys. Rev. C **23**, 920 (1981).

<sup>12</sup>I. Ragnarsson *et al.*, Nucl. Phys. **A347**, 287 (1980).

<sup>13</sup>J. Dudek *et al.*, Phys. Lett. **112B**, 1 (1982).

<sup>14</sup>Y. Schutz *et al.*, Phys. Rev. Lett. **48**, 1534 (1982).

<sup>15</sup>B. M. Nyako *et al.*, Phys. Rev. Lett. **52**, 507 (1984).

<sup>16</sup>A. Pakkanen *et al.*, Phys. Rev. Lett. **48**, 1530 (1982).

<sup>17</sup>M. A. Riley *et al.*, Proceedings of the Vth Nordic Conference on Nuclear Physics, Jyväskylä, March 1984 (to be published).

<sup>18</sup>F. S. Stephens (private communication).

<sup>19</sup>F. Azgui *et al.*, GSI International, Darmstadt, Report No. GSI-84-31.

<sup>20</sup>J. Simpson *et al.*, Phys. Rev. Lett. **53**, 648 (1984).

<sup>21</sup>Z. Szymański, in *Fast Nuclear Rotation* (Clarendon, Oxford, 1983), p. 147 ff.

<sup>22</sup>C. Baktash *et al.*, Phys. Rev. Lett. (to be published).

<sup>23</sup>J. Ragnarsson *et al.*, Lund Report No. LUND-MPH-84/12.